RESEARCH ARTICLE

MRI-ARSACS: An Imaging Index for Autosomal Recessive Spastic Ataxia of Charlevoix-Saguenay (ARSACS) Identification Based on the Multicenter PROSPAX Study

Alessandra Scaravilli, MD,[1] Davide Negroni, MD,[1] Claudio Senatore, MD,[1] Lorenzo Ugga, MD, PhD,[1] Mirco Cosottini, MD,[2] Ivana Ricca, MD, PhD,[3] Benjamin Bender, MD,[4] Andreas Traschütz, MD, PhD,[5,6] Ayşe Nazli Başak, PhD,[7] Atay Vural, MD, PhD,[8] Bart P. van de Warrenburg, MD, PhD,[9] Alexandra Durr, MD,[10] Roberta La Piana, MD, PhD,[11,12] Dagmar Timmann, MD,[13] PROSPAX Consortium, Rebecca Schüle, MD,[6,14,15] Matthis Synofzik, MD,[5,6] Filippo Maria Santorelli, MD, PhD,[3] and Sirio Cocozza, MD, PhD[1*]

[1]*Department of Advanced Biomedical Sciences, University of Naples "Federico II", Naples, Italy*
[2]*Department of Translational Research on New Technologies in Medicine and Surgery, University of Pisa, Pisa, Italy*
[3]*Department of Molecular Medicine, IRCCS Stella Maris Foundation, Pisa, Italy*
[4]*Department of Diagnostic and Interventional Neuroradiology, University of Tübingen, Germany*
[5]*Division Translational Genomics of Neurodegenerative Diseases, Center for Neurology and Hertie Institute for Clinical Brain Research, University of Tübingen, Tübingen, Germany*
[6]*German Center for Neurodegenerative Diseases (DZNE), Tübingen, Germany*
[7]*Translational Medicine Research Center, KUTTAM-NDAL, Koç University, Istanbul, Turkey*
[8]*Department of Neurology, Koç University, Istanbul, Turkey*
[9]*Department of Neurology, Donders Institute for Brain, Cognition, and Behaviour, Radboud University Medical Center, Nijmegen, The Netherlands*
[10]*ICM, Inserm, CNRS, AP-HP, Paris Brain Institute, Sorbonne University, Paris, France*
[11]*Department of Neurology and Neurosurgery, Montreal Neurological Institute, McGill University, Montreal, Quebec, Canada*
[12]*Department of Diagnostic Radiology, McGill University, Montreal, Quebec, Canada*
[13]*Department of Neurology and Center for Translational Neuro- and Behavioral Sciences (C-TNBS), Essen University Hospital, Essen, Germany*
[14]*Division of Neurodegenerative Diseases, Department of Neurology, Heidelberg University Hospital and Faculty of Medicine, Heidelberg, Germany*
[15]*Center for Neurology and Hertie Institute for Clinical Brain Research, University of Tübingen, Tübingen, Germany*

ABSTRACT: Background: Autosomal recessive spastic ataxia of Charlevoix-Saguenay (ARSACS) and hereditary spastic paraplegia type 7 (SPG7) represent the most common genotypes of spastic ataxia (SPAX). To date, their magnetic resonance imaging (MRI) features have only been described qualitatively, and a pure neuroradiological differential diagnosis between these two conditions is difficult to achieve.

Objectives: To test the performance of MRI measures to discriminate between ARSACS and SPG7 (as an index of common SPAX disease).

Methods: In this prospective multicenter study, 3D-T1-weighted images of 59 ARSACS (35.4 ± 10.3 years, M/F = 33/26) and 78 SPG7 (54.8 ± 10.3 years, M/F = 51/27) patients of the PROSPAX Consortium were analyzed, together with 30 controls (45.9 ± 16.9 years, M/F = 15/15). Different linear and surface measures were evaluated. A receiver operating characteristic analysis was performed, calculating area under the curve (AUC) and corresponding diagnostic accuracy parameters.

Results: The pons area proved to be the only metric increased exclusively in ARSACS patients ($P = 0.02$). Other different measures were reduced in ARSACS and SPG7 compared with controls (all with $P \leq 0.005$). A cut-off value equal to 1.67 of the pons-to-superior vermis area ratio proved to have the highest AUC (0.98, diagnostic accuracy 93%, sensitivity 97%) in discriminating between ARSACS and SPG7.

This is an open access article under the terms of the Creative Commons Attribution License, which permits use, distribution and reproduction in any medium, provided the original work is properly cited.

***Correspondence to:** Dr. S. Cocozza, Department of Advanced Biomedical Sciences, University "Federico II", Via Pansini 5, 80131 Naples, Italy; E-mail: sirio.cocozza@unina.it

Relevant conflicts of interest/financial disclosures: B.B. is co-founder, shareholder, and head of product development (CTO) of AIRAmed GmbH. S.C. has received advisory board fees from Amicus. None of the other co-authors have any financial conflicts of interest to declare.
Funding agencies: This project was supported as part of the PROSPAX consortium under the frame of EJP RD, the European Joint Programme on Rare Diseases, under the EJP RD COFUND-EJP No. 825575 and Deutsche Forschungsgemeinschaft (DFG, German Research Foundation) (No. 441409627). F.M.S. and I.R. are supported by RC5x1000 of the Italian Ministry of Health. A.T., M.S., and R.S. were supported by the Clinician Scientist programme "PRECISE.net" funded by the Else Kröner-Fresenius-Stiftung. B.P.vdW. is supported by ZonMw (The Netherlands Organization for Scientific Research; 463002002).

[Correction added after first online publication on 02 August 2025. The copyright line has been updated.]

Received: 13 February 2024; **Revised:** 22 April 2024; **Accepted:** 13 May 2024

Published online 7 June 2024 in Wiley Online Library (wileyonlinelibrary.com). DOI: 10.1002/mds.29871

Conclusions: Evaluation of the pons-to-superior vermis area ratio can discriminate ARSACS from other SPAX patients, as exemplified here by SPG7. Hence, we hereby propose this ratio as the Magnetic Resonance Index for the Assessment and Recognition of patients harboring SACS mutations (MRI-ARSACS), a novel diagnostic tool able to identify ARSACS patients and useful for discriminating ARSACS from other SPAX patients undergoing MRI. © 2024 The Author(s). *Movement Disorders* published by Wiley Periodicals LLC on behalf of International Parkinson and Movement Disorder Society.

Key Words: ARSACS; SPG7; biomarker; magnetic resonance imaging; ataxia

Spastic ataxia (SPAX) is a clinical phenotype defined by the coexistence of cerebellar ataxia and spastic paraplegia comprising a heterogeneous group of predominantly hereditary conditions.[1,2] Among these, autosomal recessive spastic ataxia of Charlevoix-Saguenay (ARSACS) and hereditary spastic paraplegia type 7 (SPG7) represent the most common genetic forms of SPAXs worldwide.[2,3] From a clinical perspective, these two conditions share, as expected, some similarities, such as the association between cerebellar symptoms and spasticity, but also some differences, mainly with respect to other clinical features that might be more predominant in one condition compared with the other.[4,5]

Genetic testing is, obviously, mandatory to reach the final diagnosis in SPAX patients,[6] with powerful tools such as next-generation sequencing methods that are increasingly available to neurologists working in this field.[7] Nonetheless, the daily clinical implementation of these methods is still limited to only a relatively few tertiary care centers worldwide, mostly due to their high costs.[8] Furthermore, interpretation of variants and in some cases the technical challenges in their identification[9] still represent a limitation to the full clinical implementation of this method in clinical practice. In view of this, in the early workup of these patients MRI plays a central role, being a widely accessible diagnostic tool always performed not only to exclude possible acquired causes of the observed SPAX phenotype, but also to assist the physician in both guiding and interpreting the appropriate genetic testing.[10]

Conventional MRI findings in hereditary ataxias can pose a challenge to neuroradiologists, given the presence of non-specific and sometimes overlapping imaging findings.[10] With reference to infratentorial volumetric changes that can be observed and evaluated in clinical practice, ARSACS seems to represent a peculiar condition, in which together with an expected (for a neurodegenerative disorder) volume loss affecting the cerebellum, with a more prominent involvement of the superior vermis, a volumetric increase of the pons associated with a "bulky" appearance has been reported.[10] Conversely, SPG7 patients usually show mostly unremarkable volumetric changes in the posterior fossa, with only in some cases a mild atrophy of the cerebellum, again affecting mostly the superior vermis.[10] Nevertheless, all these data come from the analyses of small cohorts of patients, limiting the identification of possible neuroradiological measures to discriminate between these two conditions.

Given this background, the aim of this study was to evaluate the diagnostic accuracy of MRI measures of infratentorial structures to differentiate ARSACS from another exemplary, frequent SPAX disease (namely, SPG7), focusing on structures reported or expected to be significantly involved in these two conditions. We tested the performance of these measures, alone and in combination, with the aim of identifying MRI measures able to achieve a neuroradiological diagnosis of ARSACS compared with other SPAXs, using SPG7 as a common proxy of these diseases. To fulfill these aims, we analyzed data acquired within the PROSPAX Consortium (PROSPAX - An integrated multimodal progression chart in spastic ataxias) (Appendix), an international, multicenter, collaborative, research project on SPAXs,[11] that has amassed in the past 3 years the largest collection of standardized clinical and MRI data of ARSACS and SPG7 patients.

Methods

Compliance with Ethical Standards

This study was conducted using data acquired within the multicenter project "An integrated multimodal progression chart in spastic ataxias" (PROSPAX) (ClinicalTrials.gov No. NCT04297891), approved by the local ethics committee of each center in accordance with the ethical standards of the institutional research committee and with the 1964 Helsinki Declaration and its later amendments. Written informed consent was obtained from each patient prior to enrollment.

Participants

In this multicenter, prospective study, data from 119 ARSACS patients, 141 SPG7 patients, and 65 healthy controls (HC) collected from January 2021 to October 2022 in eight different worldwide centers (Supplementary Materials in Data S1) were considered for inclusion. Inclusion criteria for patients were: absence of contraindication to undergo a brain MRI scan, and genetically confirmed ARSACS or SPG7. Similar inclusion criteria were applied to controls, except for the latter (ie, genetic diagnosis) and with the addition of no history of neurological or psychiatric disorders. For all groups, exclusion criteria were: presence of

contraindication or unwillingness to undergo a brain MRI scan, and presence of motion artifacts with poor quality of the images.

For each patient, a neurological examination was performed within 1 month of MRI acquisition, including assessment of disease severity with the Friedreich's Ataxia Rating Scale (FARS) Functional Stage,[12] the Scale for the Assessment and Rating of Ataxia (SARA),[13] and the Spastic Paraplegia Rating Scale (SPRS).[14]

MRI Data Acquisition and Analysis

All participants underwent the acquisition of a standardized MRI protocol using a 3 T scanner, including a high-resolution (voxel size ≤1 mm^3) 3D T1-weighted volume acquired in a sagittal plane. A list of all the scanners used at each site, together with main sequence information, is provided in Table 1, while a complete list of all sequence parameters is reported in the Supplementary Materials in Data S1.

One trained reader with more than 3 years of experience in neuroimaging (Reader A, D.N.) evaluated all the MR images blinded to the subjects' demographic, group, and clinical data. Both linear and surface variables were collected in the same midsagittal T1-weighted image, in the original subject space, as described below.

For the linear measurements (Fig. 1A), three variables were recorded[15]: the antero-posterior (AP) mid-sagittal diameter of the pons (measured tracing a line passing through the middle of the pons at the point of its maximum width, parallel to the lines used for the surface analysis – see below), the AP diameter of the vermis (collected tracing a line passing through the fastigium), and the cranio-caudal (CC) diameter of the vermis (tracing a line from the most superior to the most inferior portion of the vermis).

Similarly, three surface measures (Fig. 1B) were recorded as follows: the pons surface (defined as the area inside two straight lines traced to pass (1) through the superior pontine notch and inferior edge of the quadrigeminal plate and (2) parallel to the first line to pass through the inferior pontine notch[16]), the superior and the inferior vermis surfaces (defined as the area above or below, respectively, a line passing through the fastigium and the primary fissure).

Given that the current literature suggests the abovementioned pontine "bulky" appearance as a suggestive volumetric MRI feature of ARSACS,[10] once identified, the metric that proved to have the best diagnostic performance among the six variables collected was combined (in the form of a ratio) with the corresponding pontine measure (linear or surface, depending on the outcome of the analysis) to test if their combined evaluation would lead to a better diagnostic accuracy.

To assess both the intra- and inter-reader reliability of these MRI measures, as well as to evaluate a possible effect of the degree of experience in performing such analyses, an evaluation of a subgroup of one-third of the entire population (ie, 56 subjects randomly selected) was performed after a wash-out period of 30 days by Reader A (to assess intra-reader reliability), and independently by two board-certified neuroradiologists with more than 5 (Reader B, A.S.) and 15 years of experience (Reader C, L.U.) in neuroradiology, respectively.

Finally, a post-hoc analysis was performed in this subgroup to evaluate a possible effect of image orientation, with complete methodological details as detailed in Supplementary Materials in Data S1.

Statistical Analysis

To evaluate possible differences in terms of age between ARSACS, SPG7, and HC, independent *t*-tests were performed, while differences in terms of sex were tested via chi-squared tests. An analysis of covariance (ANCOVA) with age and sex as covariates was performed to evaluate possible differences in terms of MRI variables between the different groups. A two-way mixed intraclass correlation coefficient (ICC) analysis with absolute agreement was carried out to assess both the inter- and the intra-reader agreement.[17] To compare the performance of the different measurements in discriminating between ARSACS and SPG7, a receiver operating characteristic (ROC) analysis was performed. For each variable, area under the curve (AUC) was calculated as an index of the diagnostic performance of a measure, together with corresponding cut-off according to the Youden's index statistic[18] to obtain the optimal sensitivity and specificity values. Furthermore, to take into account the possible effect of age between the groups, or scanner variability between sites, a logistic regression analysis was performed to adjust for different covariates of interest (namely age, sex, and scanner), obtaining a predicted probability value that was then entered in a ROC analysis aimed at discriminating between ARSACS and SPG7 patients.

All statistical analyses were performed by an author with significant expertise (S.C.) in using SPSS (Statistical Package for Social Science, Version 25.0; IBM, Armonk, NY, USA), with a statistical significance set for P values ≤0.008 after Bonferroni correction for multiple comparisons (0.05/6, as the number of clinical/imaging variables tested).

Results

After the application of inclusion and exclusion criteria, finally 167 subjects were included in this study, with MRI data from 59 ARSACS patients (35.4 ± 10.3 years, M/F = 33/26), 78 SPG7 (54.8 ± 10.3 years, M/F = 51/27), and 30 HC (45.9 ± 16.9 years, M/F = 15/15) being analyzed. Demographic and clinical data for the subjects included in this study are presented

TABLE 1 *Breakdown of the main magnetic resonance imaging scanner and volumetric T1-weighted volumes information of the PROSPAX Consortium*

Site	MRI scanner	Field strength (T)	Slice orientation	Voxel size (mm^3)	Slices (n)
Site 1 (Essen, Germany)	Siemens Vida	3	Sagittal	0.8 × 0.8 × 0.8	208
Site 2 (Istanbul, Turkey)	Siemens Trio	3	Sagittal	0.8 × 0.8 × 0.8	192
Site 3 (Montreal, Canada)	Siemens Prisma	3	Sagittal	0.8 × 0.8 × 0.8	192
Site 4 (Naples, Italy)	Siemens Trio	3	Sagittal	0.8 × 0.8 × 0.8	208
Site 5 (Nijmegen, The Netherlands)	Siemens Prisma	3	Sagittal	0.9 × 0.9 × 0.9	192
Site 6 (Paris, France)	Siemens Prisma	3	Sagittal	1.0 × 1.0 × 1.0	192
Site 7 (Pisa, Italy)	GE Signa	3	Sagittal	0.8 × 0.8 × 0.8	244
Site 8 (Tübingen, Germany)	Siemens Vida	3	Sagittal	0.8 × 0.8 × 0.8	208

GE (General Electric Medical System, Milwaukee, WI, USA); Siemens (Siemens Medical Systems, Erlangen, Germany).

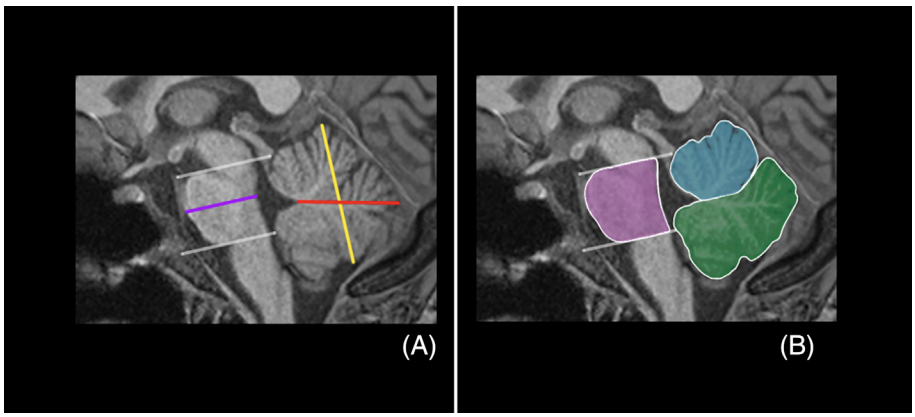


FIG. 1. Mid-sagittal T1-weighted images of a 25-year-old healthy control, with a representation of how linear (**A**) and surface measures (**B**) were evaluated. In (**A**) the craniocaudal (yellow line) and the antero-posterior diameters of the vermis (red line) are shown, together with the antero-posterior diameter of the pons (purple line) that is traced parallel to two straight lines passing through the superior and the inferior pontine notches (white lines). (**B**) An image showing how the superior (blue) and inferior (green) vermis areas were calculated, as well as the pons area (purple), defined as the surface between the abovementioned white lines. [Color figure can be viewed at wileyonlinelibrary.com]

in Table 2, with a separation by site available in the Supplementary Materials in Data S1.

The ICC analyses for the intra- and inter-reader reliability of the measurements showed an excellent agreement within readers and between readers with differing expertise (all values between 0.90 and 0.99, with the only exception of the intra-reader agreement for the AP diameter of the vermis that proved to be good, with an ICC value of 0.82– see Supplementary Materials in Data S1).

Compared with HC, both ARSACS and SPG7 patients showed a reduction in cerebellar measures (Supplementary Materials in Data S1). In particular, both AP and CC linear measures of the vermis proved to be reduced in ARSACS (23.9 ± 4.2 mm and 37.9 ± 3.7 mm, respectively) compared with HC (28.0 ± 4.3 mm and 46.2 ± 4.5 mm, respectively, both with $P < 0.001$), with a less pronounced, although still significant, reduction found in SPG7 patients (25.0 ± 3.1 mm and 43.7 ± 3.4 mm, $P = 0.005$ and $P = 0.002$, respectively). These results were confirmed when surface measures were evaluated, with a significant reduction of the superior (2.5 ± 0.5 cm^2 vs. 4.5 ± 0.7 cm^2, $P < 0.001$) and inferior (4.9 ± 0.9 cm^2 vs. 6.7 ± 1.5 cm^2, $P < 0.001$) vermian areas in ARSACS compared with HC, which was confirmed to be significant but less pronounced in SPG7 patients (4.0 ± 0.6 cm^2 and 5.7 ± 0.9 cm^2, with $P = 0.002$ for both comparisons). When ARSACS and SPG7 patients were compared, the CC measure of the vermis proved to be reduced in ARSACS patients (37.9 ± 3.7 mm vs. 43.7 ± 3.4 mm, $P < 0.001$), while no differences were seen in the AP linear measure of the vermis (23.9 ± 4.2 mm vs. 25.0 ± 3.1 mm, $P = 0.44$) between the two groups. Both vermian surfaces were significantly reduced in ARSACS patients compared with SPG7 patients, with a more prominent difference for the superior portion (2.5 ± 0.5 cm^2 vs. 4.0 ± 0.6 cm^2, $P < 0.001$) compared with the inferior portion (4.9 ± 0.9 cm^2 vs. 5.7 ± 0.9 cm^2, $P = 0.008$).

Conversely, compared with HC, ARSACS, but not SPG7, patients, showed a pontine involvement detectable

TABLE 2 *Demographic and clinical data of the study subjects*

Parameter	ARSACS (n = 59)	SPG7 (n = 78)	HC (n = 30)	*P*-value (ARSACS vs. HC)	*P*-value (SPG7 vs. HC)
Age (years)	35.4 ± 10.3 (17–63)	54.8 ± 10.3 (22–73)	45.9 ± 16.9 (17–77)	<0.001	0.001
Sex (M/F)	33/26	51/27	15/15	0.76	0.21
AAO	7.5 ± 9.5 (0–38)	36.9 ± 12.3 (2–63)	NA	NA	NA
FARS	4 (1.5–6)	3 (1–6)	0 (0–1)	NA	NA
SARA	16.5 (4–35)	11.75 (2–25)	0.5 (0–4)	NA	NA
SPRS	23 (6–44)	16 (3–38)	1 (0–5)	NA	NA

Age is reported as mean and standard deviation; clinical scores are reported as median values with corresponding ranges in parentheses.
Abbreviations: ARSACS, autosomal recessive spastic ataxia of Charlevoix-Saguenay; SPG7, hereditary spastic paraplegia type 7; HC, healthy control; M, male; F, female; AAO, age at onset; FARS, Friedreich's Ataxia Rating Scale; SARA, Scale for the Assessment and Rating of Ataxia; SPRS, Spastic Paraplegia Rating Scale; NA, not applicable.

with conventional MRI measures. In particular, while no differences in terms of linear measurements between ARSACS and HC (22.7 ± 1.5 mm vs. 22.6 ± 1.4 mm, $P = 0.79$) and SPG7 and controls (22.3 ± 1.4 mm vs. 22.6 ± 1.4 mm, $P = 0.14$) were found, when surface measures were evaluated, there was a significant increase in pons area in ARSACS patients compared with HC (5.8 ± 0.7 cm^2 vs. 5.4 ± 0.6 cm^2, $P = 0.02$); no differences were again found between SPG7 and HC (5.4 ± 0.6 cm^2 vs. 5.4 ± 0.6 cm^2, $P = 0.41$). The increase in pontine surface was confirmed in ARSACS patients also when compared with SPG7 patients, although this did not reach the statistical threshold ($P = 0.07$).

A complete list of all the measures evaluated can be found in Supplementary Materials in Data S1, together with the results of the post-hoc analysis showing the absence of a significant effect of image orientation in our analysis.

When the diagnostic performances of these measures were tested (Table 3), the best measure able to discriminate between ARSACS and SPG7 patients proved to be the superior vermis area, with an AUC of 0.97 and a sensitivity and a specificity of 95% and 83%, respectively. Given the increase in volume of the pons compared with HC in ARSACS patients, but not SPG7, when this variable was inserted in ratio with the superior vermis area, an increase in all diagnostic performance metrics was achieved. In particular, with a cut-off value of 1.67, the AUC reached a value of 0.98 (95% confidence interval: 0.96–0.99), with a sensitivity of 97% and a specificity of 90% (Table 3), corresponding to an accuracy of 93%, a positive predictive value of 88%, a negative predictive value of 97%, and a Youden's index equal to 0.86. No differences in terms of AUC were found when the analyses were corrected for age, sex, and scanner site (Supplementary Materials in Data S1).

Figure 2 illustrates the diagnostic accuracy of all the tested measures, while an example of the application of this ratio in the three different groups investigated is shown in Fig. 3.

TABLE 3 *Results of the receiver operating characteristic analyses to differentiate between autosomal recessive spastic ataxia of Charlevoix-Saguenay (ARSACS) and hereditary spastic paraplegia type 7 (SGP7) patients*

Parameter	AUC	Sensitivity (%)	Specificity (%)	Cut-off value
AP pons	0.57	52	67	22.7
AP vermis	0.63	64	67	29.0
CC vermis	0.88	83	82	40.7
Pons area	0.65	73	51	5.41
Superior vermis area	0.97	95	83	3.37
Inferior vermis area	0.74	68	67	5.25
Pons area/superior vermis area (MRI-ARSACS)	**0.98**	**97**	**90**	**1.67**

Bold type denotes the optimal cut-off value, together with the corresponding AUC, sensitivity, and specificity values, of the measure showing the best diagnostic accuracy in differentiating ARSACS from SPG7 patients.
Cut-off values for linear measures are expressed in millimeters, areas in square centimeters, with the MRI-ARSACS being a ratio and therefore adimensional.
Abbreviations: AUC, area under the curve; AP pons, antero-posterior diameter of the pons; AP vermis, antero-posterior diameter of the vermis; CC vermis, craniocaudal diameter of the vermis; MRI-ARSACS, Magnetic Resonance Index for the Assessment and Recognition of patients harboring SACS mutations.

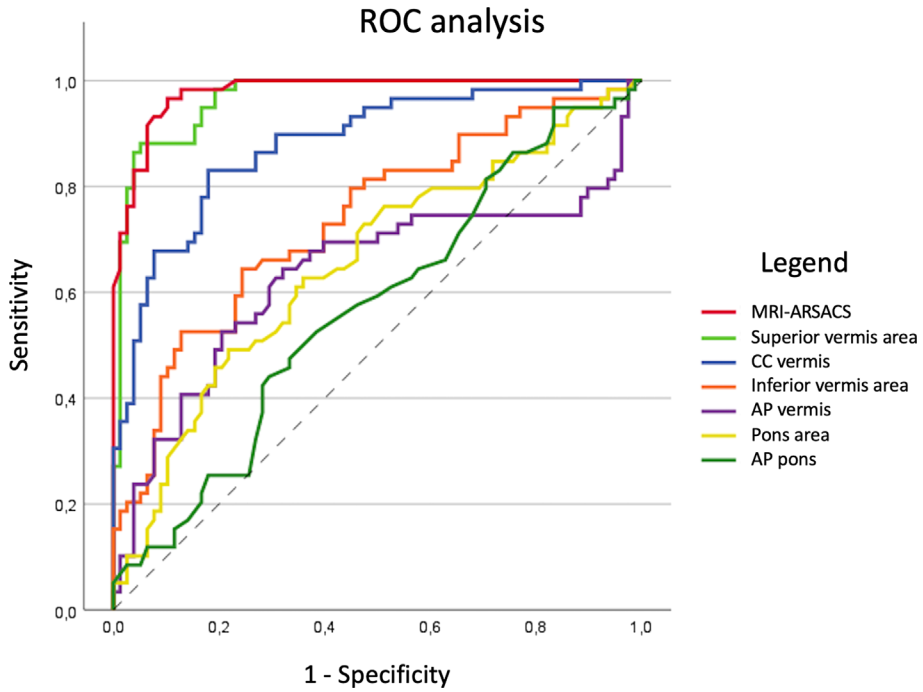


FIG. 2. Results of the receiver operating characteristic (ROC) analysis showing the highest accuracy of the Magnetic Resonance Index for the Assessment and Recognition of patients harboring SACS mutations (MRI-ARSACS) compared with the other conventional imaging metrics in discriminating between autosomal recessive spastic ataxia of Charlevoix-Saguenay (ARSACS) and hereditary spastic paraplegia type 7 patients. Abbreviations: AP pons, antero-posterior diameter of the pons; AP vermis, antero-posterior diameter of the vermis; CC vermis, craniocaudal diameter of the vermis; MRI-ARSACS, Magnetic Resonance Index for the Assessment and Recognition of patients harboring SACS mutations. [Color figure can be viewed at wileyonlinelibrary.com]

Discussion

In this study we demonstrated the high diagnostic accuracy and reliability of a conventional MRI measure in the identification of ARSACS patients compared with other forms of SPAX, using SPG7 as a model for this group of conditions. We found that a cut-off value of 1.67 of the pons-to-superior vermis area ratio can discriminate with high accuracy ARSACS from SPG7 patients, and therefore propose this measure as an imaging tool (Magnetic Resonance Index for the Assessment and Recognition of patients harboring SACS mutations – MRI-ARSACS) as a neuroradiological diagnostic tool.

Differentiating between hereditary SPAXs, especially in cases where clinical features are not typical and/or highly suggestive, is often a complex task for neuroradiologists. Indeed, from an MRI perspective, these conditions may present with very similar and, therefore, confounding features.[10] In view of this, the availability of a reliable and accurate conventional MRI measure that can easily be applied in clinical practice is, therefore, highly desirable. The neuroradiological literature contains various examples of useful MRI indices that can be helpful in the diagnosis of neurodegenerative disorders.[19-23] Of these, the Magnetic Resonance Parkinsonism Index (MRPI)[21] and its relatively recent 2.0 implementation[20] have emerged as powerful tools for differentiating progressive supranuclear palsy from other mimickers, In particular Parkinson's disease. The hereby defined MRI-ARSACS score, despite its relevance to a different group of movement disorders, shares some similarities with the MRPI. In particular, the method for the evaluation of the pons surface is the same as for the MRPI.[21] Conversely, we here introduce a new method for the separate evaluation of the superior and inferior vermis surfaces, by tracing a line passing through the fastigium and the primary fissure and calculating the areas above and below this line. Besides the use described here, we suggest that this reliable method for calculating the two portions of the cerebellar vermis might be of use in other conditions in which an apparent selection of one vermian portion over the other is more prominent, such as spinocerebellar ataxia type 7[10] or the group of diseases caused by *ITPR1* mutations (including spinocerebellar ataxia types 15 and 29[24]).

One of the possible reasons for the high diagnostic accuracy of the MRI-ARSACS reported here may lay in the peculiar "bulky" appearance of the pons consistently reported in ARSACS patients.[25,26] The mechanism behind this phenomenon is still unknown, mainly due to the scarcity of available data on

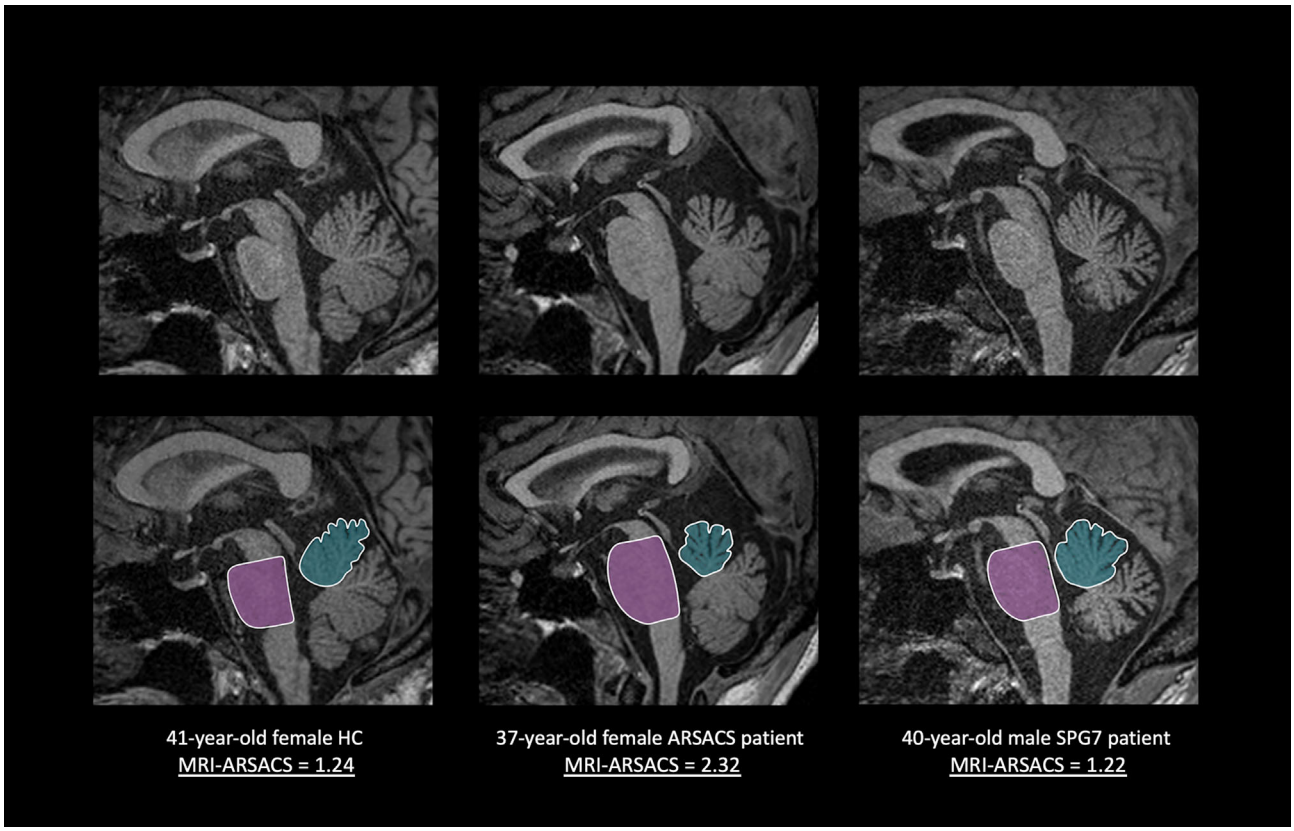


FIG. 3. Application of the Magnetic Resonance Index for the Assessment and Recognition of patients harboring SACS mutations (MRI-ARSACS) in the three groups evaluated in the present study, from left to right, a 41-year-old healthy control (HC), a 37-year-old autosomal recessive spastic ataxia of Charlevoix-Saguenay (ARSACS) patient, and a 40-year-old patient with hereditary spastic paraplegia type 7 (SPG7). [Color figure can be viewed at wileyonlinelibrary.com]

large ARSACS populations as is often the case when dealing with rare disorders. Nevertheless, based on diffusion MRI studies, this thickened pontine appearance has been suggested to be caused by, or at least associated with, an overrepresentation of latero-laterally oriented fibers of the transverse pontine fibers, as qualitatively evaluated on fractional anisotropy color maps and tractography images.[25,27,28] In line with this observation, it has also been hypothesized that the T2-hypointense stripes in the pons, another conventional imaging finding reported in ARSACS patients, might correspond to this alteration in the transverse pontine fibers.[27]

Although the pontine involvement represents therefore a central feature of ARSACS, it is noteworthy that one of the main determinants of the high diagnostic accuracy of MRI-ARSACS reflects the involvement of the superior vermis, a feature present in both SPG7 and ARSACS patients, although more prominent in the latter.[10] A possible explanation for the occurrence of this feature in ARSACS patients might be the early degeneration of Purkinje cells, as demonstrated in post-mortem studies in which a prevalent involvement of Purkinje cells in the anterior vermis, especially in the central lobule and culmen, has been reported, with a minor involvement of the cerebellar hemispheres.[29] Similarly, vermian involvement has been also demonstrated by neuropathology studies in SPG7.[30] This finding in ARSACS is also supported by a *Sacs* knockout mice model, in which the predominant involvement of Purkinje cells of the anterior lobe of the vermis was observed, followed by progressive spinal motor neuron loss and peripheral neuropathy.[31]

This study has some limitations, the first being the limited forms of SPAXs that we included in this study for further comparison. Indeed, we were able to demonstrate the efficacy of MRI-ARSACS only in distinguishing ARSACS from SPG7. Nevertheless, we would like to stress that ARSACS represents, to date, the only form of hereditary degenerative ataxia in which an increase rather than a decrease in volume of a brain region (namely the pons) is present. For this reason, we are confident that MRI-ARSACS is unlikely to fail in identifying these patients compared with other genetic causes of SPAXs, although this requires wider confirmation, especially given the heterogeneity of these conditions. A second limitation

may be the use of only linear and surface measurements. While the idea of performing a volumetric study with more sophisticated analysis methods (ie, a voxel-based morphometry study) to capture more subtle differences that might be hindered by the current manual approach is undoubtedly of interest, we focused on measurements that can be used in daily clinical practice. Finally, another limitation of the study is that we did not test how other conventional MRI signs reported in ARSACS, such as the pontine stripes, the hyperintensity of the middle cerebellar peduncles, or the thalamic rim sign,[26,32] might perform in terms of diagnostic accuracy, for different reasons. In the first instance, quantitative measurements are always more desirable compared to qualitative evaluations in all fields including neuroradiology. Furthermore, although these signs have been anecdotally reported in ARSACS patients, no information on their real incidence or on which sequences these findings should be researched (ie, axial T2-weighted vs. FLAIR sequences) has been reported to date. For this reason, future studies aimed in the first instance at understanding the exact incidence of these signs in a large and representative group of patients are warranted, before understanding whether their inclusion could help in further defining the high diagnostic accuracy of the reliable volumetric index reported here.

Despite these limitations, in conclusion we hereby propose the MRI-ARSACS as a reliable tool that is able to achieve a neuroradiological diagnosis of ARSACS, and is also able to discriminate between different SPAX phenotypes, as exemplified here by SPG7, and consequently provide a useful support to clinicians. ●

Acknowledgments: This project was supported as part of the PROSPAX Consortium under the frame of EJP RD, the European Joint Programme on Rare Diseases, under the EJP RD COFUND-EJP No. 825575 and Deutsche Forschungsgemeinschaft (DFG, German Research Foundation) (No. 441409627).

Data Availability Statement

The data that support the findings of this study are available from the corresponding author upon reasonable request.

References

1. Synofzik M, Schüle R. Overcoming the divide between ataxias and spastic paraplegias: shared phenotypes, genes, and pathways. Mov Disord 2017;32:332–345.
2. Pedroso JL, Vale TC, França Junior MC, Kauffman MA, Teive H, Barsottini OGP, et al. A diagnostic approach to spastic ataxia syndromes. Cerebellum 2021;21:1073–1084.
3. Traschütz A, Adarmes-Gomez AD, Anheim M, Baets J, Falkenburger BH, Gburek-Augustat J, et al. Autosomal recessive cerebellar ataxias in Europe: frequency, onset, and severity in 677 patients. Mov Disord 2023;38:1109–1112.
4. Ashrafi MR, Mohammadi P, Tavasoli AR, Heidari M, Hosseinpour S, Rasulinejad M, et al. Clinical and molecular findings of autosomal recessive spastic ataxia of Charlevoix Saguenay: an Iranian case series expanding the genetic and neuroimaging spectra. Cerebellum 2023;22:640–650.
5. Sáenz-Farret M, Lang AE, Kalia L, Cunha I, Sousa M, Kuhlman G, et al. Spastic paraplegia type 7 and movement disorders: beyond the spastic paraplegia. Mov Disord Clin Pract 2022;9:522–529.
6. Bagaria J, Bagyinszky E, An SSA. Genetics of autosomal recessive spastic ataxia of Charlevoix-Saguenay (ARSACS) and role of sacsin in neurodegeneration. Int J Mol Sci 2022;23:552.
7. Beijer D, Fogel BL, Beltran S, et al. Standards of NGS data sharing and analysis in ataxias: recommendations by the NGS working group of the ataxia global initiative. Cerebellum 2024;23(2):391–400.
8. Schwarze K, Buchanan J, Fermont JM, Dreau H, Tilley MW, Taylor JM, et al. The complete costs of genome sequencing: a microcosting study in cancer and rare diseases from a single center in the United Kingdom. Genet Med 2020;22:85–94.
9. Lincoln SE, Hambuch T, Zook JM, Bristow SL, Hatchell K, Truty R, et al. One in seven pathogenic variants can be challenging to detect by NGS: an analysis of 450,000 patients with implications for clinical sensitivity and genetic test implementation. Genet Med 2021;23:1673–1680.
10. Cocozza S, Pontillo G, De Michele G, Di Stasi M, Guerriero E, Perillo T, et al. Conventional MRI findings in hereditary degenerative ataxias: a pictorial review. Neuroradiology 2021;63:983–999.
11. PROSPAX—an integrated multimodal progression chart in spastic ataxias; https://www.prospax.net Accessed October 6, 2023.
12. Subramony SH, May W, Lynch D, Gomez C, Fischbeck K, Hallett M, et al. Measuring Friedreich ataxia: interrater reliability of a neurologic rating scale. Neurology 2005;64:1261–1262.
13. Schmitz-Hubsch T, Du Montcel ST, Baliko L, Berciano J, Boesch S, Depondt C, et al. Scale for the assessment and rating of ataxia: development of a new clinical scale. Neurology 2006;66:1717–1720.
14. Schule R, Holland-Letz T, Klimpe S, Kassubek J, Klopstock T, Mall V, et al. The Spastic Paraplegia Rating Scale (SPRS): a reliable and valid measure of disease severity. Neurology 2006;67:430–434.
15. Jandeaux C, Kuchcinski G, Ternynck C, Riquet A, Leclerc X, Pruvo J-P, et al. Biometry of the cerebellar vermis and brain stem in children: MR imaging reference data from measurements in 718 children. AJNR Am J Neuroradiol 2019;40(11):1835–1841.
16. Oba H, Yagishita A, Terada H, Barkovich AJ, Kutomi K, Yamauchi T, et al. New and reliable MRI diagnosis for progressive supranuclear palsy. Neurology 2005;64:2050–2055.
17. Koo TK, Li MY. A guideline of selecting and reporting intraclass correlation coefficients for reliability research. J Chiropr Med 2016;15:155–163.
18. Youden WJ. Index for rating diagnostic tests. Cancer 1950;3:32–35.
19. Oender D, Faber J, Wilke C, Schaprian T, Lakghomi A, Mengel D, et al. Evolution of clinical outcome measures and biomarkers in sporadic adult-onset degenerative ataxia. Mov Disord 2023;38:654–664.
20. Quattrone A, Morelli M, Nigro S, Quattrone A, Vescio B, Arabia G, et al. A new MR imaging index for differentiation of progressive supranuclear palsy-parkinsonism from Parkinson's disease. Parkinsonism Relat Disord 2018;54:3–8.
21. Quattrone A, Nicoletti G, Messina D, Fera F, Condino F, Pugliese P, et al. MR imaging index for differentiation of progressive supranuclear palsy from Parkinson disease and the Parkinson variant of multiple system atrophy. Radiology 2008;246:214–221.
22. Ho VB, Chuang HS, Rovira MJ, Koo B. Juvenile Huntington disease: CT and MR features. AJNR Am J Neuroradiol 1995;16(7):1405–1412.
23. Massey LA, Jager HR, Paviour DC, O'Sullivan SS, Ling H, Williams DR, et al. The midbrain to pons ratio: a simple and specific MRI sign of progressive supranuclear palsy. Neurology 2013;80:1856–1861.
24. Romaniello R, Pasca L, Panzeri E, D'Abrusco F, Travaglini L, Serpieri V, et al. Superior cerebellar atrophy: an imaging clue to diagnose *ITPR1*-related disorders. Int J Mol Sci 2022;23:6723.

25. Prodi E, Grisoli M, Panzeri M, Minati L, Fattori F, Erbetta A, et al. Supratentorial and pontine MRI abnormalities characterize recessive spastic ataxia of Charlevoix-Saguenay. A comprehensive study of an Italian series. Eur J Neurol 2013;20:138–146.

26. Synofzik M, Soehn AS, Gburek-Augustat J, Schicks J, Karle KN, Schüle R, et al. Autosomal recessive spastic ataxia of Charlevoix Saguenay (ARSACS): expanding the genetic, clinical and imaging spectrum. Orphanet J Rare Dis 2013;8:41.

27. Gazulla J, Vela AC, Marín MA, Pablo L, Santorelli FM, Benavente I, et al. Is the ataxia of Charlevoix–Saguenay a developmental disease? Med Hypotheses 2011;77:347–352.

28. Burguêz D, Oliveira CMD, Rockenbach MABC, Fussiger H, Vedolin LM, Winckler PB, et al. Autosomal recessive spastic ataxia of Charlevoix-Saguenay: a family report from South Brazil. Arq Neuropsiquiatr 2017;75:339–344.

29. Bouchard J-P, Brais B, Dupré N, Rouleau GA. Chapter 9. Hereditary ataxias and spastic parapareses in northeastern Canada. In: Brice A, Pulst SM, eds. Blue Books of Neurology. Vol. 31. Oxford, UK: Elsevier; 2007:222–243.

30. Coarelli G, Schule R, Van De Warrenburg BPC, De Jonghe P, Ewenczyk C, Martinuzzi A, et al. Loss of paraplegin drives spasticity rather than ataxia in a cohort of 241 patients with *SPG7*. Neurology 2019;92:e2679–e2690.

31. Larivière R, Gaudet R, Gentil BJ, Girard M, Conte TC, Minotti S, et al. Sacs knockout mice present pathophysiological defects underlying autosomal recessive spastic ataxia of Charlevoix-Saguenay. Hum Mol Genet 2015;24:727–739.

32. Kuchay RAH, Mir YR, Zeng X, Hassan A, Musarrat J, Parwez I, et al. ARSACS as a worldwide disease: novel SACS mutations identified in a consanguineous family from the remote tribal Jammu and Kashmir region in India. Cerebellum 2019;18:807–812.

Appendix

PROSPAX Consortium (listed in alphabetical order)

Nazan Akkaya—nakkaya20@ku.edu.tr—Koç University Translational Medicine Research Center (KUTTAM), Koc University, Istanbul, Turkey.

Murat Serhat Aygün—maygun@kuh.ku.edu.tr—Department of Radiology, Koç University, Istanbul, Turkey.

Bernard Brais—bernard.brais@mcgill.ca—Department of Neurology and Neurosurgery, Montreal Neurological Hospital and Institute, Montreal, Canada.

Paolo Cecchi—pcecchip@gmail.com—Department of Translational Research on New Technologies in Medicine and Surgery, University of Pisa, Pisa, Italy.

Giovanna De Michele—giodemic@gmail.com—Department of Neurosciences and Reproductive and Odontostomatological Sciences, University of Naples "Federico II", Naples, Italy.

Graziella Donatelli—graziella_donatelli@hotmail.com—Neuroradiology Unit, Azienda Ospedaliero-Universitaria Pisana, Pisa, Italy—Imago7 Research Foundation, Pisa, Italy.

Charlotte Dubec-Fleury—charlottedubec@hotmail.fr—Sorbonne Université, Institut du Cerveau—Paris Brain Institute-ICM, CNRS, Inria, Inserm, AP-HP, Groupe Hospitalier Sorbonne Université, Paris, France.

Sophia L. Göricke—sophia.goericke@uk-essen.de—Institute of Diagnostic and Interventional Neuroradiology, Essen University Hospital, University of Duisburg-Essen, Germany.

Christoph Kessler—christoph.kessler@uni-tuebingen.de—Department of Neurodegenerative Diseases, Center for Neurology and Hertie Institute for Clinical Brain Research, University of Tübingen, Tübingen, Germany.

Özgür Öztop-Çakmak—ooztop@ku.edu.tr—Department of Neurology, Koç University, Istanbul, Turkey.

Robin J. Palvadeau—rpalvadeau@ku.edu.tr—Koç University Translational Medicine Research Center (KUTTAM), Koç University, Istanbul, Turkey.

Sara Satolli—sara.satolli@gmail.com—Department of Molecular Medicine, IRCCS Stella Maris Foundation, Pisa, Italy.

Seyma Tekgül—stekgul@ku.edu.tr—Koç University Translational Medicine Research Center (KUTTAM), Koç University, Istanbul, Turkey.

Sophie Tezenas Du Montcel—sophie.tezenas@aphp.fr—Sorbonne Université, Institut du Cerveau—Paris Brain Institute—ICM, CNRS, Inria, Inserm, AP-HP, Groupe Hospitalier Sorbonne Université, Paris, France.

Ceren Tunca—ctunca@ku.edu.tr—Koç University Translational Medicine Research Center (KUTTAM), Koç University, Istanbul, Turkey.

Supporting Data

Additional Supporting Information may be found in the online version of this article at the publisher's web-site.